

Received June 16, 2019, accepted June 27, 2019, date of publication July 10, 2019, date of current version August 13, 2019.

Digital Object Identifier 10.1109/ACCESS.2019.2927521

Joint 3D UAV Placement and Resource Allocation in Software-Defined Cellular Networks With Wireless Backhaul

CHUNYU PAN^{1,2}, (Student Member, IEEE), JIRONG YI³, (Student Member, IEEE),
CHANGCHUAN YIN^{1,2}, (Senior Member, IEEE), JIAN YU⁴, AND XUEHUA LI¹

¹Beijing Information Science and Technology University, Beijing 100192, China

²Beijing Laboratory of Advanced Information Network, Beijing Key Laboratory of Network System Architecture and Convergence, Beijing University of Posts and Telecommunications, Beijing 100876, China

³Department of Electrical and Computer Engineering, The University of Iowa, Iowa City, IA 52242, USA

⁴Huawei Technologies Co., Ltd., Beijing 100085, China

Corresponding author: Changchuan Yin (ccyin@bupt.edu.cn)

This work was supported in part by the Beijing Natural Science Foundation and Municipal Education Committee Joint Funding Project under Grant KZ201911232046, in part by the National Natural Science Foundation of China under Grant 61671086, Grant 61629101, and Grant 61871041, and in part by the 111 Project under Grant B17007.

ABSTRACT Cellular networks assisted by flexibly placed high-maneuverability unmanned aerial vehicles (UAVs) have attracted virtual interests recently. In this paper, the utility maximization problem is investigated to determine how to improve the performance of multi-UAV enabled software-defined cellular networks (SDCNs) with wireless backhaul. The formulated problem jointly optimizes the three dimensional (3D) UAV placement, user scheduling and association, and spectrum resource allocation. The proposed problem is intractable since it is a mixed-integer combined non-convex problem. Thus, an efficient distributed alternating maximization (AM) iterative algorithm is developed to solve the proposed problem. Then, the original optimization problem is decomposed into three subproblems that are solved alternatively via the successive convex optimization (SCO) technique and the modified alternating direction method of multipliers (ADMM) in the proposed algorithm. The theoretical analysis and the simulation results confirm the convergence performance of the proposed algorithm. The extensive numerical results substantiate the superiority of the proposed algorithm, which significantly increases the throughput and utility of the overall users relative to the traditional overlaid ground base station (GBS) and UAV structure and other benchmark methods. The maximal throughput gain is as large as 74.9% on average for all users, in contrast to other benchmark schemes.

INDEX TERMS 3D UAV placement, alternating direction method of multipliers, alternating maximization, resource allocation, software-defined network, software-defined cellular network, successive convex optimization, user association.

I. INTRODUCTION

Unmanned aerial vehicles (UAVs) mounted with access points can serve as aerial base stations and form drone cells to provide additional association opportunities and resources for users in temporary or unexpected circumstances, which are expected to arise in future cellular networks [1], [2]. In these industries, some well-known information technology (IT) companies have capitalized on the growing opportunity and launched pilot aerial platform projects, such as Facebook Aquila Drone [3], Google Loon [4], and ABSOLUTE

The associate editor coordinating the review of this manuscript and approving it for publication was Daniel Benevides Da Costa.

[5], to provide wireless access. The elastic deployment of UAV networks differs from existing infrastructure in how the UAV networks connect with the core network. To provide reliable communication for UAVs, wireless backhaul and cellular-connected UAVs have recently emerged as a viable new solution since they are flexible and cost-efficient [6]–[8]. In order to improve resource utilization and the network capacity among the ground base station (GBS)-to-user links, UAV-to-user links and the UAV backhaul links in the integrated ground-air networks, future cellular networks will urgently need an efficient resource allocation strategy to elastically manage these multi-dimensional ground-air resources.

Several recent works, such as [6] and [9]–[15], have studied the use of UAVs to enhance wireless communications. By optimizing multiuser scheduling and association and UAVs' power control and trajectory, the authors in [9] maximize the minimum throughput for all users in the down-link communication. The authors in [10] derive a new fundamental energy trade-off between the UAV and its served ground terminal (GT) in throughput and energy consumption in a ground to UAV wireless communication. Under a given set of constraints on the users' minimum-rate ratio, the authors in [11] maximize the minimum average throughput of all users by jointly optimizing the UAV's trajectory and OFDMA resource allocation. In particular, the authors in [12] describe the capacity region of UAV-enabled two-user broadcast channel over a given UAV flight duration. The proposed scheme jointly optimizes the UAV trajectory and transmit power/rate allocation, subject to the maximum speed and maximum transmission power constraints of UAV. In [13], the authors consider UAVs equipped with different internet of things (IoT) devices and propose a novel interference-aware path planning scheme. The proposed scheme allows the cellular-connected UAV to minimize the interference to the ground network jointly with the transmission delay when transmitting online mission-related data. In [14], the authors determine the 3D locations of UAVs in a way that maximizes the total coverage area while maximizing the coverage lifetime of UAVs. The authors in [6] use stochastic geometry to give a performance analysis of the UAV backhaul that can be achieved by a network with dedicated ground base stations. The authors in [15] investigate how different styles of wireless backhaul with various data rates affect the number of users served by a UAV. The maximal path loss allowed in fronthaul and the constant rate backhaul are considered to maximize the number of served users by varying UAV positions in [15].

The above studies have demonstrated the performance enhancement achievable with the help of efficient UAV placement and trajectories within current cellular networks. However, many challenges occur when a drone cell is considered. First, some existing works, such as [9]–[14], have not considered reliable backhaul communications or the channel model of backhaul links for UAVs; the trajectory optimization of the two-dimensional (2D) coordinates with a fixed altitude of UAVs in [9]–[13] will lead to a sub-optimal performance within UAV-assisted cellular networks. Second, users' average performance will be ignored by the sole focus on backhaul links in [6] and no consideration of UAV-to-user links and the GBS-to-user links. Third, deploying the uncoordinated UAVs and GBS with the overlaid drone cell networks to achieve UAV-assisted communication in [6] and [15] will make the elastic networks challenging due to the lack of global network information. Meanwhile, resource allocations between different access technologies and multidimensional resources are difficult in UAV-assisted cellular networks because of their different protocols and interfaces. Accordingly, investigating flexibly UAV-assisted cellular net-

works and jointly considering the fronthaul and backhaul links requires a more fine-grained strategy; to resolve the multidimensional resource allocation problems, researchers may focus on a more intelligent scheme that can exert greater control and can be deployable in future cellular networks.

Recently, 3GPP in [16] defines the 5G system architecture and preliminarily uses techniques such as network function virtualization (NFV) and software-defined networks (SDN). The proposed architecture separates the user plane (UP) functions and the control plane (CP) functions and supports services-enabled deployments, which allows for independent scalability, evolution and flexible deployments. In [17], the authors propose a software-defined joint resource allocation and user scheduling with in-band wireless fronthaul constraints for a network consisting of locally coupled small cell base stations. In our previous work [18], we introduce software-defined cellular networks (SDCN) and formulate a weighted utility maximization problem to optimally allocate the licensed and unlicensed spectrum resource utilizing the global view of the SDCN controller. However, none of these works in [17], [18] provide a specific flexibly placed UAV-assisted structure with multiple ground-air resources. The study in [19] proposes a drone cell management framework (DMF) in cellular networks, which benefits from the cooperation of SDN, NFV and cloud computing, but the authors do not consider the details of resource allocation.

In this paper, we introduce an SDCN-based UAV-assisted architecture to satisfy the demands of future cellular networks. Taking advantage of the NFV and SDN technologies, all the wireless network components in a local geographical area (e.g., one or a small number of GBS coverage areas) are abstracted to a virtual radio access network information big-base module in the SDCN controller. To improve the performance of multi-UAV enabled software-defined cellular networks, we have formulated a resource allocation optimization problem to maximize the aggregate users' data rate utility. Based on the global view of the logical control plane in the SDCN, we investigate the joint optimal user scheduling and association, resource allocation and 3D UAV placement for the integrated ground-air cellular network for delay-tolerant services [12]. Additionally, the GBS provides the wireless backhaul for the UAVs that operate in the in-band full-duplex mode. Then, we utilize a distributed and parallel alternating maximization (AM) algorithm [20] and partition the coupled multidimensional optimization variables into three parallel blocks: the 3D UAV placement, the fronthaul and backhaul spectrum allocation, and the user scheduling and association. Finally, we successively employ the modified alternating direction method of multipliers (ADMM) [21] and successive convex optimization (SCO) [9] methods to tackle the decomposed problem in user scheduling and association and 3D UAV placement blocks. The proposed algorithm supports a centralized control logic and a distributed computational logic for future large-scale cellular networks. Theoretical analysis and numerical results reveal the convergence performance of the proposed algorithm.

In addition, the data plane can be easily reconfigured through a flow-based control signal interaction procedure according to SDN modeling, which supports the elastic characteristics of UAV-assisted schemes. The main contributions of the paper are summarized as follows:

- We perform a fundamental analysis on the UAV-to-user links, GBS-to-user links and the wireless backhaul for UAVs from GBS, including the interference between multi-UAVs and backhaul links to drone cell users. By jointly optimizing multidimensional coupled factors, such as user scheduling, 3D UAV placement and resource allocation, we maximize the overall network utility while supporting the reliable communication of flexible UAVs.
- We propose a distributed and parallel AM algorithm to partition the coupled multidimensional optimization variables into three parallel blocks, which are 3D UAV placement, fronthaul and backhaul spectrum allocation, and user scheduling and association. Then, we successively employ the SCO and the modified ADMM methods to tackle the 3D UAV placement, as well as the user scheduling and association blocks. The theoretical and the numerical results show the rapid convergence performance of the proposed algorithm.
- To alleviate the computational burden of the user scheduling and association at the SDCN controller, we design the updating operations at the SDCN controller to be simple one-time algebraic calculations. Updating at the users and the BSs (including the GBS and UAVs) are achieved concurrently. The centralized control logic and the distributed computational logic in the proposed method are suitable for the future networks with multiple access technologies.

The simulation results show that the proposed algorithm can achieve better performance with higher utility and higher throughput with regard to all network users.

The rest of this paper is organized as follows. Section II defines the system model and describes the problem formulation. Then, in Section III, we propose an efficient distributed and parallel AM algorithm to solve the resource allocation problem by employing the SCO techniques and modified ADMM. Some numerical results for the proposed technique are presented in Section IV, and our conclusions are drawn in Section V.

Notations: In this paper, we use italic letters, bold-face lower-case and upper-case letters to denote scalars, vectors and matrices, respectively. For a matrix \mathbf{Z} , $\|\mathbf{Z}\|$ represents the Euclidean norm, and its transpose is denoted by \mathbf{Z}^T . Meanwhile, $\mathbf{Z}(r)$ denotes the r th iteration of \mathbf{Z} , and $\mathbf{Z}[m]$ refers to the m -th column or m -th row of the matrix \mathbf{Z} .

II. SYSTEM MODEL AND PROBLEM FORMULATION

A. SYSTEM MODEL

We consider the downlink of a ground cellular network consisting of GBSs. Each GBS has a large number of antennas, and the number of antennas is denoted as J_t . For simplicity,

only one antenna is assumed for each user (the index of users is $S = \{1, 2, \dots, S\}$), but the proposed model in this paper is also applicable to a multi-antenna system of users. In the event of a temporary situation (such as sports, concerts, or debris), these GBSs may become inapposite to serve users. Therefore, flexibly placed UAVs can form drone cells to assist ground cellular networks, and in-demand users can associate with such UAVs. Here, we introduce a group of UAVs, i.e., $\mathcal{V} = \{1, 2, 3, \dots, V\}$, each of which has a fixed transmission power and a single antenna and operates in the full-duplex mode. The GBS provides a wireless backhaul at each UAV. Aerial drone cells and the ground cellular networks form a heterogeneous network (HetNet) composed of ground-air resources. One of the solutions for supporting these flexible networks is SDCN, which separates the data plane (DP) functions and the control plane (CP) functions and allows for independent scalability, evolution and flexible deployments [16]. In SDCN, the above-mentioned network entities, such as GBS, UAVs and users, form a logical data plane according to conventional SDN modeling [22], as shown in Fig. 1.

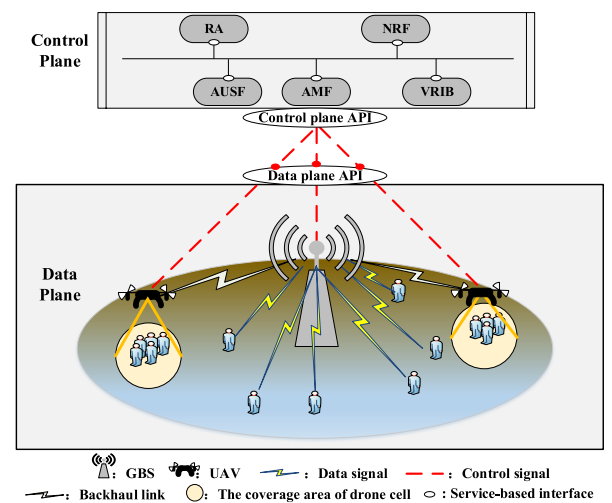


FIGURE 1. SDCN-based UAV-assisted wireless network structure.

In the logical control plane of the SDCN, the controller has a global view of the whole network [23]. It abstracts out all base stations (BSs), including GBSs and UAVs, which are deployed in a geographical area in the data plane as a virtual radio access network information big-base module (VRIB). The VRIB module considers all the physical network components, such as base stations, as simply radio elements with minimal control logic [24]. The SDCN controller application also consists of many other function modules [16], [18], [25] including the authentication server function (AUSF) module, the access and mobility management function (AMF) module, the network repository function (NRF) module and the resource allocation function (RAF) module. Once authenticated by the AUSF module, a user can access all available virtual network resources, which are owned by either ground cellular networks or drone cells and have

been mapped into the VRIB module. Then, the NRF module executes the efficient successive convex optimization for the optimal placement of the UAVs (described in Section III. A). The AMF module together with all the base stations and users execute the distributed user scheduling and association algorithm (described in Section III. B). The RAF module executes the spectrum allocation optimization for the optimal resource allocation, which is described in Section III. C. The service-based interfaces are used for the interaction among the function module services in the SDCN controller [16]. The complete SDCN framework shows that the controller utilizes the global view of the network. The proposed algorithm exploits the full knowledge of the whole network to execute the distributed network resource allocation and user scheduling and then realizes the optimal decision in the SDCN controller.

All entities in the data plane are equipped with a data plane API [24], (such as OpenFlow protocol [26], [27]) to enable the SDCN controller to easily communicate control messages through the control plane API to the network components. The complete SDCN control plane framework and the control diagram are shown in Fig. 2, where the control message is transmitted through the “service flow” [18].

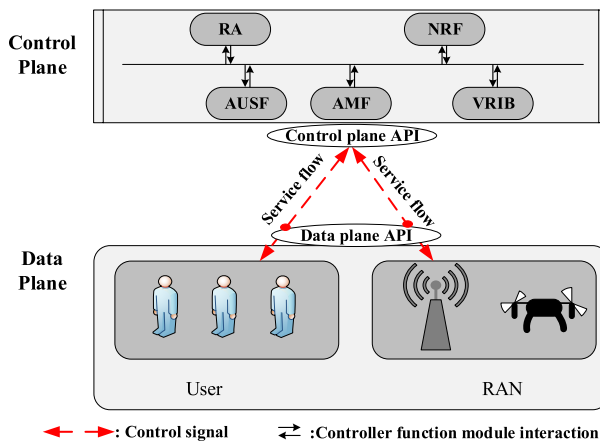


FIGURE 2. The SDCN control diagram.

In the next part, we introduce the signal models for communication among GBSs, users and UAVs.

1) THE ACHIEVABLE RATE BETWEEN GBS AND USERS

The small-scale Rayleigh fading and large-scale free-space path loss channel is considered for the terrestrial GBS-user links [28], which can be expressed as

$$h_{i0} = \tilde{h}_{i0} d_{i0}^{-\beta_1}, \quad (1)$$

where d_{i0} is the Euclidean distance between GBS and user i and $\tilde{h}_{i0} = |\mathbf{h}^{i0} \mathbf{l}^{i0}|^2$, where $\mathbf{h}^{i0} \in \mathbb{R}^{1 \times J_t}$ is the complex channel vector from GBS to user i and $\mathbf{l}^{i0} \in \mathbb{R}^{J_t \times 1}$ is the precoding vector from GBS to user i . β_1 is the path loss exponent. Then, the achievable rate between GBS and user i can be

expressed as

$$r_{i0} = y_{i0} \alpha \log_2 \left(1 + \frac{p_i^G h_{i0}}{\sigma^2} \right), \quad (2)$$

where p_i^G and σ^2 denote the transmission power of GBS and the power of the additive white Gaussian noise (AWGN) at the receiver, respectively. α is the fraction spectrum allocation of GBS users, and y_{i0} is the fraction of resources for user i served by the GBS.

2) THE ACHIEVABLE RATE OF WIRELESS BACKHAUL FROM GBS TO UAV

Assume that the altitude of the j th UAV is h_j^u . The Euclidean distance between the GBS at $(x^G, y^G, 0)$ and the UAV j at (x_j^u, y_j^u, h_j^u) is [9], [29],

$$d_{j0}^u = \sqrt{(h_j^u)^2 + (x^G - x_j^u)^2 + (y^G - y_j^u)^2}. \quad (3)$$

It is assumed that the sub-6 GHz band and LoS links for the air-to-ground channels are applied to the wireless backhaul from GBSs to UAVs. Hence, the large-scale fading of channel gain from UAV j to GBS complies with the free-space path loss model, which can be expressed as [9], [13], [29]

$$h_{j0} = \tilde{h}_{j0} d_{j0}^u^{-\beta_2}, \quad (4)$$

where $\tilde{h}_{j0} = |\mathbf{h}^{j0} \mathbf{l}^{j0}|^2$, $\mathbf{h}^{j0} \in \mathbb{R}^{1 \times J_t}$ is the complex channel vector from GBS to UAV j and $\mathbf{l}^{j0} \in \mathbb{R}^{J_t \times 1}$ is the precoding vector from GBS to UAV j . β_2 is the path loss exponent. We assume that the backhaul link transmission satisfies the zero-forcing (ZF) criterion, and thus the achievable rate of the wireless backhaul from the GBS to UAV j ($j = 1, \dots, V$) can be expressed as

$$r_{j0} = (1 - \alpha) \log_2 \left[1 + \frac{p_j^G h_{j0}}{p_j \epsilon + \sum_{k=1, k \neq j}^V p_k h_{kj} + \sigma^2} \right], \quad (5)$$

where p_j^G and p_j represent the transmission power of GBS and UAV j , respectively. h_{j0} and h_{kj} are the channel gains from the GBS to UAV k and between UAVs k and j , respectively. ϵ represents the self-cancellation ability of UAV j , which operates in full-duplex mode.

3) THE ACHIEVABLE RATE BETWEEN UAV AND USERS

Once authenticated by the AC, the two-dimensional (2D) location coordinates of each user i are known by the SDCN controller and are represented by (x_i, y_i) . The distance between UAV j at (x_j^u, y_j^u, h_j^u) and the associated user i at $(x_i, y_i, 0)$ is

$$d_{ij}^u = \sqrt{(h_j^u)^2 + (x_j^u - x_i)^2 + (y_j^u - y_i)^2}. \quad (6)$$

As mentioned above, the sub-6 GHz band and LoS links are assumed for the air-to-ground channels [9], [13]. Hence, the large-scale fading of UAV-to-user links complies with the free-space path loss model [9], [13], [29], and the ground-air channel gains UAV-to-user links can be expressed as

$$h_{ij} = \tilde{h}_{ij} d_{ij}^u^{-\beta_2} \quad (7)$$

where $\tilde{h}_{ij} = |\mathbf{h}^{ij}\mathbf{l}^{ij}|^2$, $\mathbf{h}^{ij} \in \mathbb{R}^{1 \times 1}$ is the complex channel vector from UAV j to user i , and $\mathbf{l}^{ij} \in \mathbb{R}^{1 \times 1}$ is the precoding vector from UAV j to user i . The access link for the users associated with the UAVs will receive interference from the wireless backhaul link provided by the GBS. Thus, the achievable rate between UAV j ($j = 1, \dots, V$) and user i is

$$r_{ij} = y_{ij}(1-\alpha) \log_2 \left(1 + \frac{p_j h_{ij}}{\sum_{m=1, m \neq j}^V p_m h_{im} + p^G h_{i0} + \sigma^2} \right), \quad (8)$$

where p_j and p_m are the transmission power of UAV j and UAV m , respectively, h_{im} is the channel gains from UAV m to user i , and y_{ij} is the fraction of resources of user i served by UAV j .

B. PROBLEM FORMULATION

All UAVs and GBSs are collectively called base stations (BSs) in the following for textual brevity. The association of users and BSs is defined by the binary random variables $\mathbf{O} = \{o_{ij}\}$, i.e.,

$$o_{ij} = \begin{cases} 1, & \text{user } i \text{ is associated with BS } j \\ 0, & \text{others.} \end{cases}$$

To improve the performance of multi-UAV enabled SDCN with wireless backhaul, we formulate a resource allocation optimization problem to maximize the aggregate users' utility function. It is assumed that user i obtains the utility $U(r_{ij})$ when the achievable data rate is r_{ij} . To accomplish fairness among users [30], the utility function $U(\cdot)$ is defined as a continuously differentiable, monotonically increasing, and logarithmic function, $U(\cdot) = \log_2(\cdot)$. The utility maximization problem involves finding the optimal 3D UAV placement $\{\mathbf{x}^u, \mathbf{y}^u, \mathbf{h}^u\}$, the optimal spectrum resource allocation α for GBS-user links, UAV-user links and UAV backhaul links, the optimal resource allocation $\{y_{ij}\}$ ($j = 0, 1, \dots, V$) for each user, and the user association indicators $\{o_{ij}\}$. Thus, the utility maximization problem is formulated as

$$\max_{\alpha, \mathbf{y}_{ij}, \mathbf{O}, \mathbf{x}^u, \mathbf{y}^u, \mathbf{h}^u} \sum_{i=1}^S \sum_{j=0}^V \log_2(r_{ij}), \quad (9a)$$

$$\text{subject to } o_{ij} \in \{0, 1\}, i \in \mathcal{S}, \quad j = 0, 1, \dots, V, \quad (9b)$$

$$\sum_{j=0}^V o_{ij} = 1, i \in \mathcal{S}, \quad (9c)$$

$$\sum_{i=1}^S r_{ij} \leq r_{j0}, \quad j = 1, 2, \dots, V, \quad (9d)$$

$$0 \leq \alpha \leq 1, \quad (9e)$$

$$0 \leq y_{ij} \leq 1, \quad j = 1, 2, \dots, V \quad (9f)$$

$$x_l \leq x_j^u \leq x_h, \quad (9g)$$

$$y_l \leq y_j^u \leq y_h, \quad (9h)$$

$$h_l \leq h_j^u \leq h_h. \quad (9i)$$

Constraint (9b) denotes user association indicators, and constraint (9c) indicates that each user can only associate with one BS. Since the UAVs receive the signals from the wireless backhaul link and transmit data to the associated users, the total transmission rate of each user will be decided by the wireless backhaul link, which is denoted by (9d). The constraint (9e) indicates the spectrum allocation for GBS-user links, UAV-user links and UAV backhaul links. The constraint (9f) describes the resource allocation of each user. The constraints (9g)-(9i) confine the allowed space for the UAVs to move, where h_l , x_l , y_l , h_h , x_h and y_h denote the minimum and maximum allowed values for the coordinates of h_j^u , x_j^u and y_j^u , respectively.

III. ALGORITHM DEVELOPMENT

We assume that the resources for each user associated with BSs are equally allocated, i.e., the resource in each cell is equally allocated to all effective associated users [30]. Thus, the fractional resource allocation for each user i served by BS j becomes

$$y_{ij} = \frac{1}{e_j}, \quad j = 0, 1, \dots, V, \quad (10)$$

where e_j is the number of users associated with each BS j , i.e., $e_j = \sum_i o_{ij}, j \in \{0, 1, \dots, V\}$. Thus, the problem in (9) can be reformulated as

$$\max_{\alpha, \mathbf{O}, e_j, \mathbf{x}^u, \mathbf{y}^u, \mathbf{h}^u} \sum_{i=1}^S \sum_{j=0}^V o_{ij} \log_2 \left(\frac{r'}{e_j} \right), \quad (11a)$$

$$\text{subject to } e_j = \sum_i o_{ij}, \quad i \in \mathcal{S}, \quad j = 0, 1, \dots, V, \quad (11b)$$

$$\sum_{i=1}^S o_{ij} r_{ij}' \leq e_j r_{j0}, \quad j = 1, \dots, V, \quad (11c)$$

$$(9b), (9c), (9e), (9g), (9h), (9i), \quad (11d)$$

where $r' = [r'_{i0}, r'_{ij}]$ ($j = 1, 2, \dots, V$), and

$$r'_{i0} = \alpha \log_2 \left(1 + \frac{p_i^G h_{i0}}{\sigma^2} \right),$$

$$r'_{ij} = (1 - \alpha) \log_2 \left(1 + \frac{p_j h_{ij}}{\sum_{m=1, m \neq j}^V p_m h_{im} + p^G h_{i0} + \sigma^2} \right).$$

Constraint (11b) describes the number of users associated with each BS j , and constraint (11c) is from (9d).

The binary variables o_{ij} assume integer values and give rise to combinatorial problems; this issue is typically circumvented by relaxing them into a continuous constraint [18], [30]. Then, problem (11) can be rewritten as

$$\max_{\alpha, \mathbf{O}, \mathbf{x}^u, \mathbf{y}^u, \mathbf{h}^u, e_j} \sum_{i=1}^S \sum_{j=0}^V o_{ij} \log_2 \left(\frac{r'}{e_j} \right), \quad (12a)$$

$$\text{subject to } 0 \leq o_{ij} \leq 1, \quad \forall i, j, \quad (12b)$$

$$(11b), (11c), (9c), (9e), (9g), (9h), (9i). \quad (12c)$$

Even when we relax the integer variables, the above optimization problem is still combinatorial and non-convex, as it needs to search I) over many coupled optimization dimensions, such as 3D UAV placement, user association indicators and resource allocation, as well as II) over the non-convex fraction item in the objective function and constraint (11c). In general, there is no standard method for directly solving such non-convex problems efficiently. In this paper, we propose an efficient AM iterative algorithm for problem (12) by applying the SCO technique and modified ADMM method. Specifically, we update the variables \mathbf{O} , $\{\mathbf{x}^u, \mathbf{y}^u, \mathbf{h}^u\}$, and α alternatively. Given an initialization of these variables, we update the 3D UAV placement $\{\mathbf{x}^u, \mathbf{y}^u, \mathbf{h}^u\}$ with the other variables fixed. Then, we update the resource allocation α with the rest of the variables fixed. Finally, we update the user scheduling and association \mathbf{O} with the other variables fixed. The above process repeats until a stopping criterion is met.

A. 3D UAV PLACEMENT OPTIMIZATION IN THE NRF MODULE

For given $\{o_{ij}\}$ and α , the 3D UAV placement of problem (12) in the NRF module can be reformulated as

$$\begin{aligned} & \max_{\mathbf{x}^u, \mathbf{y}^u, \mathbf{h}^u} \sum_{i=1}^S \left(o_{i0} \log_2 \left(\alpha \log_2 (1 + \phi_{i0}) \right) / e_0 \right) \\ & + \sum_{j=1}^V o_{ij} \log_2 \left((1 - \alpha) \log_2 (1 + \phi_{ij}) \right) / e_j \right), \end{aligned} \quad (13a)$$

$$\text{subject to } \sum_{i=1}^S o_{ij} (1 - \alpha) \log_2 (1 + \phi_{ij}) \leq e_j (1 - \alpha) \log_2 (1 + \phi_{j0}), \quad j = 1, \dots, V, \quad (13b)$$

$$x_l \leq x_j^u \leq x_h, \quad (13c)$$

$$y_l \leq y_j^u \leq y_h, \quad (13d)$$

$$h_l \leq h_j^u \leq h_h. \quad (13e)$$

where we have

$$\phi_{i0} = \frac{p_i^G h_{i0}}{\sigma^2},$$

$$\phi_{ij} = \frac{\frac{p_j \tilde{h}_{ij}}{(h_j^u)^2 + (x_j^u - x_i)^2 + (y_j^u - y_i)^2}}{\sum_{m=1, m \neq j}^V \frac{p_m \tilde{h}_{im}}{(h_m^u)^2 + (x_m^u - x_i)^2 + (y_m^u - y_i)^2} + p^G h_{i0} + \sigma^2},$$

$$\phi_{j0} = \frac{\frac{p^G \tilde{h}_{j0}}{(h_j^u)^2 + (x_j^u - x^G)^2 + (y_j^u - y^G)^2}}{\sum_{k=1, k \neq j}^V \frac{p_k^G \tilde{h}_{k0}}{(h_k^u)^2 + (x_k^u - x^G)^2 + (y_k^u - y^G)^2} + p_j \epsilon + \sigma^2},$$

and constraint (13b) is from (11c).

Remark 1: Problem (13) is a non-convex non-concave problem.

To solve the intractable problem (13), we employ an efficient SCO technique [9] and extend the method to the 3D UAV placement optimization. First, we define an intermediate variable $\mathbf{Z}[m] \triangleq [h_m^u, x_m^u, y_m^u]^T (m = 1, 2, \dots, V)$

and rewrite the coordinates of ground users and the GBSs as the matrix form, which are $\mathbf{C}^u[i] \triangleq [0, x_i, y_i]$ and $\mathbf{C}^G \triangleq [0, x^G, y^G]$. Then, the achievable data rate r_{ij} from UAV j ($j = 1, 2, \dots, V$) to user i ($i = 1, 2, \dots, S$) can be rewritten as

$$\begin{aligned} r_{ij} &= y_{ij}(1 - \alpha) \log_2 (1 + \phi_{ij}) \\ &= (1 - \alpha) \left(\hat{r}_{ij} - \log_2 \left(\sum_{m=1, m \neq j}^V \frac{p_m \tilde{h}_{im}}{\|\mathbf{Z}[m] - \mathbf{C}^u[i]\|^2} \right. \right. \\ &\quad \left. \left. + p^G h_{i0} + \sigma^2 \right) \right), \end{aligned} \quad (14)$$

where

$$\hat{r}_{ij} = \log_2 \left(\sum_{j=1}^V \frac{p_j \tilde{h}_{ij}}{\|\mathbf{Z}[j] - \mathbf{C}^u[i]\|^2} + p^G h_{i0} + \sigma^2 \right).$$

Similarly, the achievable data rate of wireless backhaul from the GBS to UAV j ($j = 1, 2, \dots, V$) can be rewritten as

$$\begin{aligned} r_{j0} &= (1 - \alpha) \log_2 (1 + \phi_{j0}) \\ &= (1 - \alpha) \left(\hat{r}_{j0} - \log_2 \left(\sum_{k=1, k \neq j}^V \frac{p^G \tilde{h}_{j0}}{\|\mathbf{Z}[k] - \mathbf{C}^G\|^2} + p_j \epsilon + \sigma^2 \right) \right), \end{aligned} \quad (15)$$

where

$$\hat{r}_{j0} = \log_2 \left(\sum_{j=1}^V \frac{p^G \tilde{h}_{j0}}{\|\mathbf{Z}[j] - \mathbf{C}^G\|^2} + p_j \epsilon + \sigma^2 \right).$$

According to eqs. (14) and (15), the problem (13) can be reformulated as problem (16), which is

$$\begin{aligned} & \max_{\mathbf{Z}} \sum_{i=1}^S \left(o_{i0} \log_2 \left(\alpha \log_2 (1 + \phi_{i0}) \right) / e_0 \right) \\ & + \sum_{j=1}^V o_{ij} \log_2 \left((1 - \alpha) \left(\hat{r}_{ij} - \log_2 \left(\sum_{m=1, m \neq j}^V \frac{p_m \tilde{h}_{im}}{\|\mathbf{Z}[m] - \mathbf{C}^u[i]\|^2} \right. \right. \right. \\ & \quad \left. \left. \left. + p^G h_{i0} + \sigma^2 \right) \right) / e_j \right), \end{aligned} \quad (16a)$$

$$\begin{aligned} & \text{subject to } \sum_{i=1}^S o_{ij} (1 - \alpha) \left(\hat{r}_{ij} - \log_2 \left(\sum_{m=1, m \neq j}^V \frac{p_m \tilde{h}_{im}}{\|\mathbf{Z}[m] - \mathbf{C}^u[i]\|^2} \right. \right. \\ & \quad \left. \left. + p^G h_{i0} + \sigma^2 \right) \right) \\ & \leq e_j (1 - \alpha) \left(\hat{r}_{j0} - \log_2 \left(\sum_{k=1, k \neq j}^V \frac{p^G \tilde{h}_{j0}}{\|\mathbf{Z}[k] - \mathbf{C}^G\|^2} \right. \right. \\ & \quad \left. \left. + p_j \epsilon + \sigma^2 \right) \right), \end{aligned} \quad (16b)$$

$$x_l \leq x_j^u \leq x_h, \quad (16c)$$

$$y_l \leq y_j^u \leq y_h, \quad (16d)$$

$$h_l \leq h_j^u \leq h_h, \quad (16e)$$

In the following, we utilize the SCO technique in each iteration to approximately solve problem (16). It can be verified that \hat{r}_{ij} is convex with respect to $\|\mathbf{Z}[j] - \mathbf{C}^u[i]\|^2$ [9]. Note that the convex function at any point has a global lower bound from its first-order Taylor expansion. Then, we achieve the lower bound according to the following steps:

- 1) Give a point $\mathbf{Z}[j](n_1)$ in the n_1 -th iteration.
- 2) With the first-order Taylor expansion at the given local point $\mathbf{Z}[j](n_1)$ according to [9], we obtain the lower bound \hat{r}_{ij}^l of \hat{r}_{ij} as

$$\begin{aligned}\hat{r}_{ij} &\triangleq \log_2 \left(\sum_j^V \frac{p_j \tilde{h}_{ij}}{\|\mathbf{Z}[j] - \mathbf{C}^u[i]\|^2} + p^G h_{i0} + \sigma^2 \right) \\ &\geq \sum_{j=1}^V -A_{ij}(n_1) \left(\|\mathbf{Z}[j] - \mathbf{C}^u[i]\|^2 - \|\mathbf{Z}[j](n_1) - \mathbf{C}^u[i]\|^2 \right) \\ &\quad + B_{ij}(n_1) \\ &\triangleq \hat{r}_{ij}^l,\end{aligned}\quad (17)$$

where $A_{ij}(n_1)$ and $B_{ij}(n_1)$ ($i \in \mathcal{S}, j = 1, \dots, V$) are constants that can be given by

$$A_{ij}(n_1) = \frac{\frac{p_j \tilde{h}_{ij}}{(\|\mathbf{Z}[j](n_1) - \mathbf{C}^u[i]\|^2)^2} \log_2(e)}{\sum_{l=1}^V \frac{p_l \tilde{h}_{il}}{\|\mathbf{Z}[l](n_1) - \mathbf{C}^u[i]\|^2} + p^G h_{i0} + \sigma^2}, \quad (18)$$

$$B_{ij}(n_1) = \log_2 \left(\sum_{l=1}^V \frac{p_l \tilde{h}_{il}}{\|\mathbf{Z}[l](n_1) - \mathbf{C}^u[i]\|^2} + p^G h_{i0} + \sigma^2 \right), \quad (19)$$

where p_l is the transmission power of UAV l and \tilde{h}_{il} is the channel power from UAV l to user i .

- 3) Define

$$\varphi = (1 - \alpha) \left(\hat{r}_{ij}^l - \log_2 \left(\phi_{im} + p^G h_{i0} + \sigma^2 \right) \right), \quad (20)$$

where $\phi_{im} = \sum_{m=1, m \neq j}^V \frac{p_m \tilde{h}_{im}}{\|\mathbf{Z}[m] - \mathbf{C}^u[i]\|^2}$, and the slack variables $\mathcal{T} = \left\{ \mathbf{T} : T_{ij} = \|\mathbf{Z}[j] - \mathbf{C}[i]\|^2 \right\}$, $i \in \mathcal{S}, j = 0, 1, \dots, V$. Then, with the given local point $\mathbf{Z}[j](n_1)$ and the lower bound \hat{r}_{ij}^l , problem (16) can be approximated as

$$\max_{\mathbf{T}, \mathbf{Z}, \varphi} \sum_{i=1}^S \left(o_{i0} \log_2 \left(\alpha \log_2 (1 + \phi_{i0}) / e_0 \right) + \sum_{j=1}^V o_{ij} \log_2 (\varphi / e_j) \right), \quad (21a)$$

$$\text{subject to } \sum_{i=1}^S o_{ij} \varphi \leq e_j (1 - \alpha) \left(\hat{r}_{j0}^l - \log_2 \left(\sum_{k=1, k \neq j}^V \frac{p_k^G \tilde{h}_{kj}}{T_{k0}} + p_j \epsilon + \sigma^2 \right) \right), \quad (21b)$$

$$\begin{aligned}\varphi &= (1 - \alpha) \left(\hat{r}_{ij}^l - \log_2 \left(\sum_{m=1, m \neq j}^V \frac{p_m \tilde{h}_{im}}{\|\mathbf{Z}[m] - \mathbf{C}^u[i]\|^2} + p^G h_{i0} + \sigma^2 \right) \right),\end{aligned}\quad (21c)$$

$$\mathcal{T} = \left\{ \mathbf{T} : T_{ij} = \|\mathbf{Z}[j] - \mathbf{C}[i]\|^2 \right\}, \quad (21d)$$

$$x_l \leq x_j^u \leq x_h, \quad (21e)$$

$$y_l \leq y_j^u \leq y_h, \quad (21f)$$

$$h_l \leq h_j^u \leq h_h, \quad (21g)$$

where $T_{k0} = \|\mathbf{Z}[k] - \mathbf{C}^G\|^2$. Note that problem (21) is a convex problem with the concave constraint (21b)-(21d) and the linear constraints (21e)-(21g) and can be solved by many off-the-shelf tools, such as CVX [9], [31] and the interior point method [31]. By solving problem (21), we obtain a newer local point $\mathbf{Z}[j](n_1 + 1)$ and then plug the newer local point into steps 1)-3) for the next computation until convergence. The optimal 3D UAV placement can be obtained from $\mathbf{Z}[j]$ with steps 1)-3). Thus, the complexity of SCO is the sum of the cost of first-order Taylor expansion and the interior point method. Specifically, we analytically evaluated the lower bound \hat{r}_{ij}^l of \hat{r}_{ij} with the first-order Taylor expansion at the given point $\mathbf{Z}[j](n_1)$, and the cost of the first-order Taylor expansion can be reduced to simple algebraic substitution and linear operations. The cost of the first-order Taylor expansion in our case can be negligible compared to the cost of the interior point method. Thus, the complexity of SCO is based on the complexity analysis of the interior-point method for solving convex conic optimization problems. Specifically, problem (21) invokes V second order cone constraints of size 5, $2SV$ second order cone constraints of size 7 [11], SV second order cone constraints of size 4, $6V$ linear inequality constraints of size 1, where the total number of variables is $3V + 2$. According to the analytical expression in [32], the total calculation complexity for solving problem (21) by SCO method is $(147V^3 + 48SV^2)\sqrt{(6S + 7V)}$.

B. SPECTRUM ALLOCATION OPTIMIZATION IN THE RAF MODULE

With given user association indicators $\{o_{ij}\}$, and UAV placement coordinates $\{\mathbf{x}^u, \mathbf{y}^u, \mathbf{h}^u\}$, we optimize α by solving the following optimization problem:

$$\max_{\alpha} \sum_{i=1}^S \left(o_{i0} \log_2 (\alpha c_{i0}) + \sum_{j=1}^V o_{ij} \log_2 ((1 - \alpha) c_{ij}) \right), \quad (22a)$$

$$\text{subject to } 0 \leq \alpha \leq 1, \quad (22b)$$

where

$$c_{i0} = \frac{\log_2 \left(1 + \frac{p_i^G h_{i0}}{\sigma^2} \right)}{\sum_{i=1}^S o_{i0}},$$

and

$$c_{ij} = \frac{\log_2 \left(1 + \frac{p_j h_{ij}}{\sum_{m=1, m \neq j}^V p_m h_{im} + p^G h_{i0} + \sigma^2} \right)}{\sum_{i=1}^S o_{ij}}, \quad j = 1, \dots, V.$$

Let \mathcal{F} denote the objective function (22a). Note that \mathcal{F} is twice differentiable, that is, its second derivative $\frac{\partial^2 \mathcal{F}}{\partial \alpha^2}$ exists,

which is

$$\frac{\partial^2 \mathcal{F}}{\partial \alpha^2} = -\frac{\sum_{i=1}^S o_{i0}}{\alpha^2 \ln 2} - \frac{\sum_{i=1}^S \sum_{j=1}^V o_{ij}}{(1-\alpha)^2 \ln 2}, \quad (23)$$

where o_{ij} is the given binary integer variable, $\alpha^2 \geq 0$ and $(1-\alpha)^2 \geq 0$. Then, we have $\frac{\partial^2 \mathcal{F}}{\partial \alpha^2} \leq 0$, and the objective function (22a) is a concave function. As constraint (22b) is linear, we obtain the optimal value of α from $\frac{\partial \mathcal{F}}{\partial \alpha} = 0$ in the convex problem (22), which is

$$\alpha = \frac{\sum_{i=1}^S o_{i0}}{\sum_{i=1}^S \sum_{j=1}^V o_{ij} + \sum_{i=1}^S o_{i0}}. \quad (24)$$

C. THE DISTRIBUTED USER SCHEDULING AND ASSOCIATION

For given UAV placement $\{\mathbf{x}^u, \mathbf{y}^u, \mathbf{h}^u\}$ and resource allocation α , the user scheduling and association subproblem of problem (12) can be expressed as

$$\max_{o_{ij}, e_j} \sum_i \sum_j o_{ij} \log_2(r') - \sum_j e_j \log_2(e_j), \quad (25a)$$

$$\text{subject to } \sum_{j=0}^V o_{ij} = 1, \quad \forall i, \quad (25b)$$

$$0 \leq o_{ij} \leq 1, \quad \forall i, j, \quad (25c)$$

$$\sum_{i=1}^S o_{ij} = e_j, \quad \forall j, \quad (25d)$$

$$\sum_{i=1}^S o_{ij} r'_{ij} \leq e_j r_{j0}, \quad j = 1, 2, \dots, V, \quad (25e)$$

The constraint (25d) indicates the number of users served by the BS, and the constraint (25e) is from (11c).

Remark 2: Problem (25) is a convex problem.

Thus, problem (25) can be rewritten as

$$\min_{o_{ij}, e_j} - \sum_i \sum_j o_{ij} \log_2(r') + \sum_j e_j \log_2(e_j), \quad (26a)$$

$$\text{subject to } \sum_{j=0}^V o_{ij} = 1, \quad \forall i, \quad (26b)$$

$$0 \leq o_{ij} \leq 1, \quad \forall i, j, \quad (26c)$$

$$\sum_{i=1}^S o_{ij} = e_j, \quad \forall j, \quad (26d)$$

$$\sum_{i=1}^S o_{ij} r'_{ij} \leq e_j r_{j0}, \quad j = 1, 2, \dots, V. \quad (26e)$$

Then, we use the modified fully distributed ADMM algorithm [18], [21], [33] to solve problem (26). The computing paradigm of the proposed algorithm is shown in Fig. 3 and can be described as follows. During each iteration, the BSs and users update \mathbf{O} and \mathbf{e} concurrently. The updated \mathbf{O} and \mathbf{e} are gathered by the SDCN controller, which performs a simple algebraic update on Λ (described in Eq. (27)) and

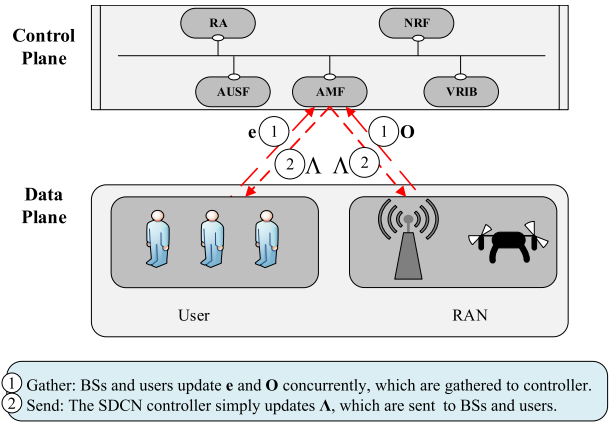


FIGURE 3. Schematic representation of the computing paradigm for distributed user scheduling and association.

sends the variables Λ back to the BSs and users for user association and scheduling. The iteration repeats until the optimal values of the association indicators are obtained. In particular, we first calculate the partial and augmented Lagrangian of problem (26) [18], [33], which introduces the Lagrange multipliers $\Lambda = [\lambda_j^a, \lambda_j^b]$ only for constraints (26d) and (26e).

$$\begin{aligned} \mathcal{L}(\mathbf{O}, \mathbf{e}, \Lambda) &= - \sum_i \sum_j o_{ij} \log_2(r') + \sum_j e_j \log_2(e_j) \\ &\quad - \sum_j \lambda_j^a (\sum_i o_{ij} - e_j) - \sum_j \lambda_j^b (\sum_{i=1}^S o_{ij} r'_{ij} - e_j r_{j0}) \\ &\quad + \frac{\rho_1}{2} \left\| \sum_i o_{ij} - \mathbf{e} \right\|^2 + \frac{\rho_2}{2} \left\| \sum_i o_{ij} r'_{ij} - \mathbf{e}^T \mathbf{r}^0 \right\|^2, \end{aligned} \quad (27)$$

where $\mathbf{r}^0 = [r_{j0}]$, and ρ_1 and ρ_2 are the augmented Lagrangian parameters. The updates for the associated number of users within the UAVs and the associated indicators of all BSs can be performed concurrently on the basis of ADMM.

1) BS UPDATE FOR THE NUMBER OF ASSOCIATED USERS
At each BS j , the update rule for the number of associated users can be expressed as

$$\begin{aligned} e_j(n_2 + 1) &= \operatorname{argmin}_{e_j} \left(\sum_j e_j \log_2(e_j) \right. \\ &\quad \left. + (\rho_1/2) \left(\sum_i o_{ij}(n_2) - e_j + \lambda_j^a(n_2) \right)^2 \right. \\ &\quad \left. + (\rho_2/2) \left(\sum_i o_{ij}(n_2) r'_{ij} - e_j r_{j0} + \lambda_j^b(n_2) \right)^2 \right), \end{aligned} \quad (28)$$

where $\sum_i o_{ij}(n_2) + \lambda_j^a(n_2)$ and $\sum_i o_{ij}(n_2) r'_{ij} + \lambda_j^b(n_2)$ are the control signals sent from the SDCN controller to the BSs. During each round of updates, the BSs send e_j to the

SDCN controller. Note that the update in Eq. (28) is a small-scale unconstrained convex optimization problem and can be solved by many off-the-shelf tools, such as CVX [31]. The update of each BS j is calculated locally and performed independently.

2) USER UPDATE FOR THE ASSOCIATION INDICATORS

At each user, the update rule for the association indicators can be expressed as

$$\begin{aligned} o_{ij}(n_2 + 1) = \operatorname{argmin}_{o_{ij}} & \left(-\sum_i \sum_j o_{ij} \log_2(r') \right. \\ & + (\rho_1/2) \left(\sum_i o_{ij} - e_j(n_2 + 1) + \lambda_j^a(n_2) \right)^2 \\ & \left. + (\rho_2/2) \left(\sum_i o_{ij} r' - e_j(n_2 + 1) r_{j0} + \lambda_j^b(n_2) \right)^2 \right), \end{aligned} \quad (29a)$$

$$\text{subject to } \sum_{j=0}^V o_{ij} = 1, \quad \forall i, \quad (29b)$$

$$0 \leq o_{ij} \leq 1, \quad \forall i, j \quad (29c)$$

where $-e_j(n_2 + 1) + \lambda_j^a(n_2)$ and $-e_j(n_2 + 1) r_{j0} + \lambda_j^b(n_2)$ are the control signals sent from the SDCN controller to the users. During each round of updates, the users send o_{ij} to the SDCN controller. It is known that the update in problem (29) is a small-scale convex optimization problem with a linear constraint and can be solved by off-the-shelf tools, such as CVX [31]. Additionally, the update of each user i is calculated locally and performed independently, which makes the update process secure.

3) THE AMF MODULE OF THE SDCN CONTROLLER UPDATE

At the AMF module of the SDCN controller, the update rule is

$$\lambda_j^a(n_2 + 1) = \lambda_j^a(n_2) + \sum_i o_{ij}(n_2 + 1) - e_j(n_2 + 1), \quad (30)$$

$$\lambda_j^b(n_2 + 1) = \lambda_j^b(n_2) + \sum_i o_{ij}(n_2 + 1) r'_{ij} - e_j(n_2 + 1) r_{j0}. \quad (31)$$

After gathering o_{ij} and e_j from the BSs and users, the AMF module in the SDCN controller performs a simple update of the dual variable λ_j^a and λ_j^b by algebraic operation. Then, the control signals (described in Section III-C. 1 and 2) are sent back to the BSs and users.

Note that the calculation complexity of modified ADMM here is the sum of the cost of the e_j -update ($j = 0, 1, \dots, V$), the cost of the o_{ij} -update ($i = 1, \dots, S, j = 0, 1, \dots, V$) and the cost of the Lagrange multipliers' update in each iteration [21]. In this paper, the e_j -update and the o_{ij} -update are unconstrained convex optimization and convex optimization problem with linear constraint, respectively. The cost of the unconstrained convex optimization is much less than the cost of the constrained convex optimization. In addition, the updates of the Lagrange multipliers in Eqs. (30) and (31)

are simple algebraic substitution and linear operations, and the cost can be negligible compared to the costs listed above. Thus, the computational complexity of the modified ADMM in this paper is decided by o_{ij} -update, which is solved by CVX [31] invoking the interior point method. Specifically, the o_{ij} -update invokes S linear inequality constraints of size 1 [11], $2S(V + 1)$ linear inequality constraints of size 1, where the total number of variables is $S(V + 1)$. According to the analytical expression in [32], the total calculation complexity for the o_{ij} -update is $2S^2V^2\sqrt{S(2V + 1)}$. Thus, the total complexity of modified ADMM algorithm is $O(S^{\frac{5}{2}}V^{\frac{5}{2}})$ in this paper.

D. UAV-ASSISTED RESOURCE ALLOCATION IN SDCN-BASED NETWORKS WITH WIRELESS BACKHAUL

The proposed algorithm is described in Algorithm 1. Meanwhile, in order to ensure the convergence of the ultimate scheme, the initialization of the horizontal UAV placement follows the circle packing scheme [9], [35]. An example of a circle packing initialization scheme with 3 circles is shown in Fig. 4. It can intuitively be seen from Fig. 4 that the circles correspond to the initial horizontal coordinates and the coverage of each UAV can be sufficiently separated to minimize the multi-UAV co-channel interference. Meanwhile, all circles together may cover the entire area in demand as much as possible to better balance the user association and the user rate. Thus, in our case, the complexity of AM is the sum of the cost of $\{\mathbf{x}^u, \mathbf{y}^u, \mathbf{h}^u\}$ -update, the cost of α -update, and the cost of \mathbf{O} -update. Then, we treat the iteration of the AM algorithm as an external iteration and the iteration of each block as an internal iteration, i.e., the iterations in ADMM and SCO are referred to as internal iterations. In the proposed algorithm,

Algorithm 1 UAV-Assisted Distributed Alternating Maximization Iterative Algorithm in SDCN-Based Networks

Initialization: $\mathbf{O}(0), \alpha(0), \mathbf{x}^u(0), \mathbf{y}^u(0), \mathbf{h}^u(0), \rho_1 > 0, \rho_2 > 0;$

- 1: **Repeat**
- 2: Solve problem (16) in the NRF module of the SDCN controller for a given $\{\alpha(r), \mathbf{O}(r)\}$ and denote the optimal solution as $\{\mathbf{x}^u(r+1), \mathbf{y}^u(r+1), \mathbf{h}^u(r+1)\}$;
- 3: Obtain the optimal value of $\{\alpha(r+1)\}$ in eq. (24) in the RAF module of the SDCN controller for a given $\{\mathbf{x}^u(r+1), \mathbf{y}^u(r+1), \mathbf{h}^u(r+1)\}, \mathbf{O}(r)$ and $\{\alpha(r)\}$;
- 4: For a given $\{\mathbf{x}^u(r+1), \mathbf{y}^u(r+1), \mathbf{h}^u(r+1)\}, \{\alpha(r+1)\}$ and $\mathbf{O}(r)$, the BSs and users update \mathbf{e} (in problem (28)) and \mathbf{O} (in problem (29)) concurrently, and the SDCN controller updates Λ . Denote the optimal solution as $\{\mathbf{O}(r+1)\}$;
- 5: Update $r = r + 1$;
- 6: **Until** the residual between the two consecutive iterations is below a threshold ι .

Output: $\mathbf{x}^u, \mathbf{y}^u, \mathbf{h}^u, \mathbf{O}, \alpha$.

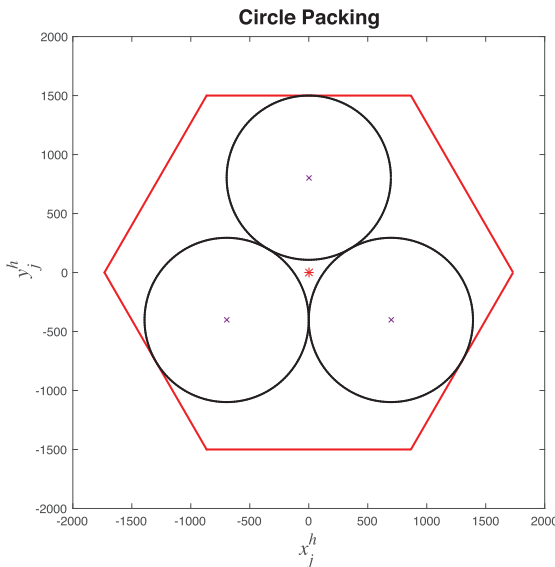


FIGURE 4. Example of UAV placement initialization with circle packing: The black solid lines and the purple cross at the center of each circle are the results obtained from the circle packing scheme, which are the coverage and the initialization horizontal coordinates of each UAV, respectively. The solid red lines are the initial GBS coverage, and the red asterisk indicates the location of the GBS.

the $\{\mathbf{x}^u, \mathbf{y}^u, \mathbf{h}^u\}$ -update is achieved by the SCO method, and the \mathbf{O} -update is achieved by the modified ADMM method in each external iteration. As shown before, the complexity of the SCO method for $\{\mathbf{x}^u, \mathbf{y}^u, \mathbf{h}^u\}$ -update and the complexity for \mathbf{O} -update are $O((147V^3 + 48SV^2)\sqrt{(6S + 7V)})$ and $O(S^{\frac{5}{2}}V^{\frac{5}{2}})$, respectively. The updates of α are simple algebraic substitution and linear operations with the analytic solutions, and the cost can be negligible compared to the costs listed above. Thus, the total complexity of AM in each external iteration is $O((147V^3 + 48SV^2)\sqrt{(6S + 7V)} + S^{\frac{5}{2}}V^{\frac{5}{2}})$. The convergence performance is given by Fig. 10 in Section IV.

Note that each blocks of the AM algorithm needs to exchange information in the SDCN controller to enable the alternate and parallel iterations. First, in the $(r + 1)$ -th iteration, the NRF module of the SDCN controller will execute the 3D UAV placement optimization based on the given $o_{ij}(r)$ and $\alpha(r)$ and then send the optimal $\{\mathbf{x}^u(r + 1), \mathbf{y}^u(r + 1), \mathbf{h}^u(r + 1)\}$ to the RAF module and AMF module. The information overhead from NRF to RAM and AMF in this iteration is $6V$ (the size of $\{\mathbf{x}^u(r + 1), \mathbf{y}^u(r + 1), \mathbf{h}^u(r + 1)\}$). Based on $\{\mathbf{x}^u(r + 1), \mathbf{y}^u(r + 1), \mathbf{h}^u(r + 1)\}$ and given $o_{ij}(r)$, the RAF module will obtain the optimal value of $\{\alpha(r + 1)\}$ in eq. (24) in the RA module of the SDCN controller for the given $\{\mathbf{x}^u(r + 1), \mathbf{y}^u(r + 1), \mathbf{h}^u(r + 1)\}$, $\mathbf{O}(r)$ and $\{\alpha(r)\}$ and then send the optimal $\{\alpha(r + 1)\}$ to the NRF module and AMF module. The information overhead from NRF to RAM and AMF in this iteration is 2 (the size of $\alpha(r + 1)$). Finally, in the $(r + 1)$ -th iteration, the AMF module will obtain the optimal $o_{ij}(r + 1)$ based on the $\{\mathbf{x}^u(r + 1), \mathbf{y}^u(r + 1), \mathbf{h}^u(r + 1)\}$ and $\alpha(r + 1)$ and then send the optimal $o_{ij}(r + 1)$ to the NRF module and AMF module, respectively. The information overhead from AMF to NRF and RAM in

this iteration is $2SV$ (the size of $o_{ij}(r + 1)$). In addition, the information overhead between the AMF module of the SDCN controller to BSs and users in ADMM is $V(3S + 1)$ (the size of Λ , o_{ij} and e_j for control messages gathering and sending). The sizes of the information exchange are quite small compared to the data body and can be communicated in the dedicated control channel [33].

IV. SIMULATION RESULTS

In this section, we provide the numerical results and the corresponding examples to demonstrate the effectiveness of the proposed algorithm. In the simulations, GBS is placed at the center of its coverage area, with a radius of 500 m. There are S users that are randomly spread in the region of GBS with a uniform distribution. The receiver noise power is assumed to be $\sigma^2 = -110$ dBm [9], and the path loss exponent $\beta_1 = \beta_2 = 2$. The transmission power of UAVs is assumed to be $p_j = 1$ W [34], and the transmission power of GBSs is $p^G = 40$ W [14]. Meanwhile, the channel power gains at the reference distance $d_0 = 1$ m are 0.1 W, and the residual threshold of the proposed algorithm is $\iota = 10^{-4}$ [9]. There are $V = 3$ UAVs adopted in the simulation. The range of UAV coordinates is $x_l = -1500, x_h = 1500, y_l = -1500, y_h = 1500$, and $h_l = 50$ m, $h_h = 500$ m. The biasing factors of GBS and UAV are $\{a_{GBS}, a_{UAV}\} = \{1.00, 1.88\}$ in the rate bias [30]. We repeat the experiment for 1000 different trials, and the corresponding system setup will change according to the locations of users generated in each trial.

A. THE THROUGHPUT AND UTILITY PERFORMANCE OF USERS

In Figs. 5 and 6, we compare the cumulative distribution function (CDF) of the user throughput and the utility of all users ($S = 8$) in the following three cases. The CDF $F(\mathbf{X})$ displays a plot of the empirical CDF for the data in the matrix \mathbf{X} . The empirical CDF $F(\mathbf{X})$ is defined as the proportion of data values less than or equal to the maximum number of elements in a matrix \mathbf{X} .

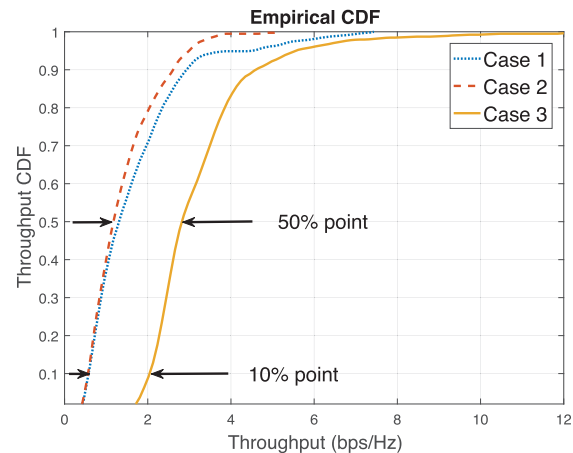


FIGURE 5. The CDFs of overall user throughput in the integrated GBS and UAV networks.

- Case 1 (Optimal 3D UAV placement with resource allocation in the traditional overlay structure): With the optimal 3D UAV placement, this case employs a fixed resource allocation in the traditional networks where the UAV and GBS are overlaid. The user association is obtained by the k-nearest neighbor (KNN) method.
- Case 2 (Optimal resource allocation with static UAV placement in the SDCN-based structure): This case is obtained by the circle packing initialization scheme, and each UAV is statically placed at the geometric center of each circle [9]. The resource in this case is optimally allocated in the SDCN, and the rounding method is adopted to restore the single BS association [30].
- Case 3 (Optimal resource allocation with optimal 3D UAV placement in the SDCN-based structure): In this case, we implement the optimal algorithm according to the utility maximization problem studied in Sections II and III in the UAV-assisted SDCN. For the values between 0 and 1 of o_{ij} , the rounding method is adopted to revert to a single BS association.

It is observed from Figs. 5 and 6 that the proposed optimal resource allocation with optimal 3D UAV placement in the SDCN-based structure in case 3 has the best throughput and utility performance compared with cases 1 and 2. Additionally, the performance gains are $\{74.9\%, 70.5\%\}$ and $\{57.1\%, 52.8\%\}$ for the 10th percentile throughput and 50th percentile throughput marked with double arrows compared with cases 1 and 2 from Fig. 5. The gains comparison of the two data points indicates that the proposed optimal method can improve the average throughput of overall users, and it is more beneficial to the users on the edge of the network. Apart from the SDCN controller's global view of all network resources, this finding is due mainly to the joint optimization of 3D UAV placement, user association and resource allocation, which improves the throughput and utility of users. Then, the distributed method can decrease the control overhead of the centralized controller and can optimize multiple resources in a parallel way, which improves the efficiency of searching for the optimal solution in the overall network.

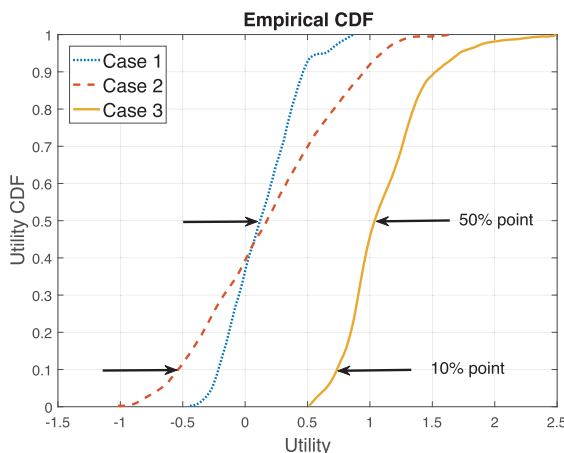


FIGURE 6. The CDFs of overall user utility in the integrated GBS and UAV networks.

The gains of the proposed schemes can be compared for the different UAV placement benchmark strategies mentioned in Cases 1 and 2. Furthermore, the proposed scheme to investigate the optimal resource allocation is the optimal 3D UAV placement scheme and can be proven superior by considering the optimal resource allocation in a 2D UAV placement strategy with a fixed altitude. Figs. 7 and 8 demonstrate the throughput and utility of overall users with the proposed optimal scheme and the optimal resource allocation in the scenario of this paper for 2D UAV placement in the fixed 100 m altitude [9]. We consider cases with different number of users. It can be seen from the two figures that the proposed algorithm can obtain better throughput and utility performance compared with the optimal 2D UAV placement. Meanwhile, the gains of the proposed optimal scheme increase as the number of users increases. The reason is that the proposed algorithm can guarantee the maximization of users' utility and the throughput with the optimal 3D UAV placement as the users' location changes, while the fixed altitude will lead to sub-optimal performance by the users.

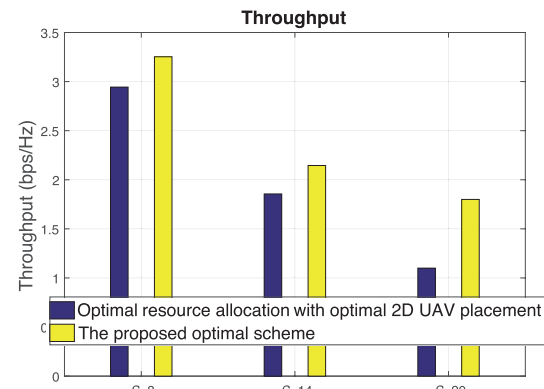


FIGURE 7. Overall user throughput in integrated GBS and UAV networks when ($S = 8$, $S = 14$) and ($S = 20$).

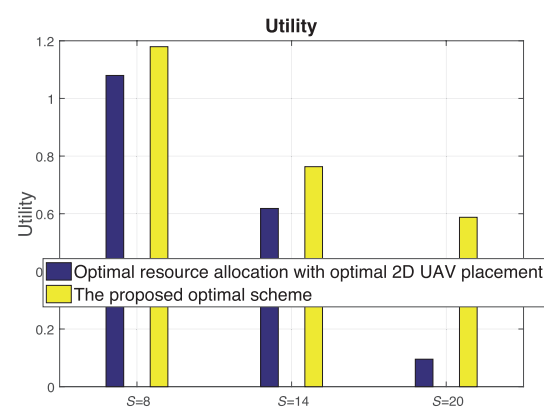


FIGURE 8. The overall user utility in the integrated GBS and UAV networks when ($S = 8$, $S = 14$) and ($S = 20$).

B. THE AVERAGE NUMBER OF USERS ASSOCIATED WITH EACH UAV

Fig. 9 compares the average number of associated users with each UAV for the schemes of the static placed UAV and the optimal placed UAV (which is case 3 in Section IV. A).

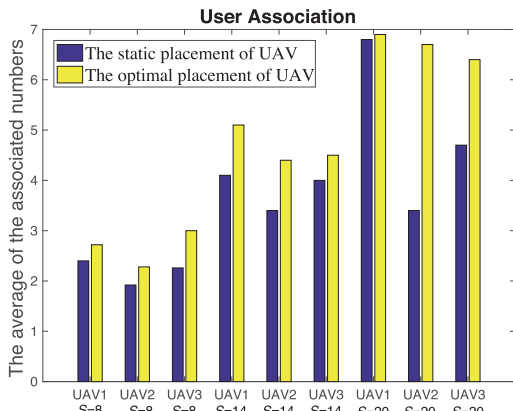


FIGURE 9. The average number of users associated with each UAV when ($S = 8$), ($S = 14$) and ($S = 20$).

The static placing scheme is obtained by the circle packing initialization scheme, and each UAV is statically placed at the geometric center of each circle in each simulation trial. Fig. 9 indicates that the optimal placed UAV always serves more users than the other schemes. Meanwhile, with the increase in the number of users, the proposed optimal placed scheme will obtain a more balanced association distribution of each UAV, which is mainly because the optimal placed scheme can figure out the user association and resource allocation in a real-time mode with changes in users' location and state in each simulation trial. In addition, the proposed optimal scheme satisfies users' real-time performance demands with the optimal user association and scheduling.

C. CONVERGENCE PERFORMANCE

We study the convergence performance of the proposed optimal algorithm in terms of the residual norm in Fig. 10. The residual norm is defined as the norm of the difference between the r -th iterative value and the prior iterative (i.e., $(r - 1)$ -th iterative) value of optimal variables [21]. Note that we have three residual norms for the variables, which are coordinates of UAVs, user scheduling and association, and resource allocation. Thus, we take the maximum residual norm among the three variables. For better readability,

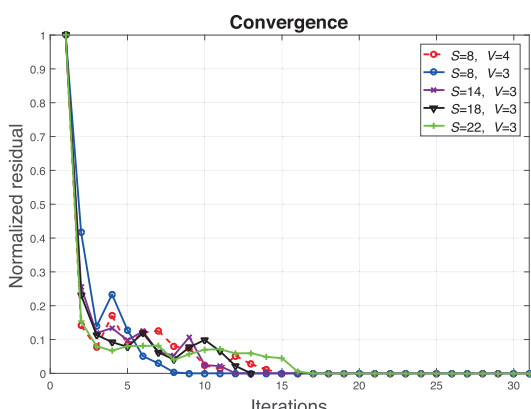


FIGURE 10. Convergence performance of the proposed optimal algorithm by residual norm in different number of users and UAVs.

we normalize the maximal residual to 1 for the convergence performance. Fig. 10 indicates that the residual norm of the optimal variables reduces to zero for different numbers of users and UAVs after a moderate number of iterations, and the proposed algorithm ensures a fast convergence. It also shows that it takes a longer time for the proposed algorithm in $S = 22$, $V = 3$ to converge compare with $S = 8$, $V = 3$, $S = 14$, $V = 3$ and $S = 18$, $V = 3$. In addition, Fig. 10 also indicates that the algorithm needs more iterations when the number of UAVs increases with the same number of users (e.g., $S = 8$, $V = 3$ and $S = 8$, $V = 4$). The reason is that when more users and UAVs exist in the network, more time is needed for the SDCN controller to coordinate BSs and users for an optimal allocation of the resource. Thus, the proposed algorithm can be performed efficiently for future wireless networks with a rational number of users and UAVs according to the convergence.

V. CONCLUSION

In this paper, utilizing a global view of the SDCN controller, we propose an SDCN-based distributed resource allocation algorithm in the new type of multi-UAV-assisted cellular networks with wireless backhaul. Benefiting from the flexible SDCN structure, the real-time perception and update of multi-dimensional variables, such as user association and scheduling, 3D UAV placement and the fronthaul and backhaul spectrum allocation are jointly optimized by the maximization of data rate utility among overall users. The formulated problem is intractable since it is a mixed integer and non-convex problem. Thus, we exploit an efficiently distributed and parallel maximization (AM) iterative algorithm to solve the proposed original problem. The coupled multiple optimization variables are partitioned into three parallel blocks in the algorithm. Then, the successive convex optimization (SCO) and the modified alternating direction method of multipliers (ADMM) techniques make the problem of 3D UAV placement and user scheduling and association blocks more tractable. The numerical results and the analysis demonstrate that the SDCN-based distributed optimal resource allocation algorithm in the multi-UAV-assisted cellular networks offers superior performance improvement over the traditional separated GBS and UAV schemes, and the maximal throughput gains can be as large as 74.9% for the overall users.

APPENDIX A

PROOF OF REMARK 1

First, the objective function in Eq. (13a) can be rewritten as

$$\begin{aligned} & \sum_{i=1}^S \left(o_{i0} \log_2 \left(\alpha \log_2(1 + \phi_{i0}) / e_0 \right) \right. \\ & \quad \left. + \sum_{j=1}^V o_{ij} \log_2 \left((1 - \alpha) \log_2(1 + \phi_{ij}) / e_j \right) \right), \\ & = R_{i0} + \sum_{j=1}^V o_{ij} \log_2 \left((1 - \alpha) \log_2(1 + \phi_{ij}) / e_j \right), \end{aligned} \quad (32)$$

where $R_{i0} = \sum_{i=1}^S \left(o_{i0} \log_2 \left(\alpha \log_2(1 + \phi_{i0}) / e_0 \right) \right)$ is a constant in problem (13) for the variables $\{\mathbf{x}^u, \mathbf{y}^u, \mathbf{h}^u\}$. Based on ϕ_{ij} , Eq. (32) can be further rewritten as

$$\begin{aligned} R_{i0} &+ \sum_{j=1}^V o_{ij} \log_2 \left((1 - \alpha) \log_2(1 + \phi_{ij}) / e_j \right) \\ &= R_{i0} + \sum_{j=1}^V o_{ij} \log_2 \left((1 - \alpha) \right. \\ &\quad \times \log_2 \left(\frac{\sum_{j=1}^V \frac{p_j \tilde{h}_{ij}}{(h_j^u)^2 + (x_j^u - x_i)^2 + (y_j^u - y_i)^2} + p^G h_{i0} + \sigma^2}{\sum_{m=1, m \neq j}^V \frac{p_m \tilde{h}_{im}}{(h_m^u)^2 + (x_m^u - x_i)^2 + (y_m^u - y_i)^2} + p^G h_{i0} + \sigma^2} \right) \\ &= R_{i0} + R_{ij} + R_{im}, \end{aligned} \quad (33)$$

where

$$\begin{aligned} R_{ij} &= \sum_{j=1}^V o_{ij} \log_2 \left((1 - \alpha) \right. \\ &\quad \times \log_2 \left(\sum_{j=1}^V \frac{p_j \tilde{h}_{ij}}{(h_j^u)^2 + (x_j^u - x_i)^2 + (y_j^u - y_i)^2} \right. \\ &\quad \left. \left. + p^G h_{i0} + \sigma^2 \right) \right), \quad j \in (1, \dots, V), \end{aligned}$$

and

$$\begin{aligned} R_{im} &= \sum_{j=1}^V o_{ij} \log_2 \left((1 - \alpha) \right. \\ &\quad \times \log_2 \left(\sum_{m=1, m \neq j}^V \frac{p_m \tilde{h}_{im}}{(h_m^u)^2 + (x_m^u - x_i)^2 + (y_m^u - y_i)^2} \right. \\ &\quad \left. \left. + p^G h_{i0} + \sigma^2 \right) \right), \quad m \in (1, \dots, V) \end{aligned}$$

and $m \neq j$.

As mentioned above, we define $\mathbf{Z}[j] \triangleq [h_j^u, x_j^u, y_j^u]^T$ ($j = 1, 2, \dots, V$), which are the variables in R_{ij} . In addition, we define $\mathbf{K}[m] \triangleq [h_m^u, x_m^u, y_m^u]^T$ ($m = 1, 2, \dots, V$) to describe the variables in R_{im} . Then, we give the serialization of variables \mathbf{Z} and \mathbf{K} by defining $\mathbf{D} = [Z_{11}, Z_{12}, Z_{13}, \dots, Z_{V1}, Z_{V2}, Z_{V3}, K_{11}, K_{12}, K_{13}, \dots, K_{V1}, K_{V2}, K_{V3}]^T$ with $\mathbf{D} \in \mathbb{R}^{6V}$. Since there are no coupling terms for Z_{ij} and K_{im} in the objective function in Eq. (13a), only the diagonal elements exist in the Hessian matrix. Thus, the Hessian matrix in Eq. (13a) with \mathbf{D} is

$$\mathbf{H}_2^{hessian} = \begin{bmatrix} -\frac{2}{\ln a} & & & & & \\ & \ddots & & & & \\ & & -\frac{2}{\ln a} & & & \\ & & & \frac{2}{\ln a} & & \\ & & & & \ddots & \\ & & & & & \frac{2}{\ln a} \end{bmatrix} \quad (34)$$

with $\mathbf{H}_2^{hessian} \in \mathbb{R}^{6V}$. Note that $\mathbf{H}_2^{hessian}$ is an indefinite matrix, and thus Eq. (13a) is a non-convex non-concave function. Similarly, constraint (13b) is a non-convex constraint. Thus, we conclude that problem (13) is a non-convex non-concave problem.

APPENDIX B

PROOF OF REMARK 2

For any given UAV placement $\{\mathbf{x}^u, \mathbf{y}^u, \mathbf{h}^u\}$ and resource allocation α , problem (25) is only used to achieve the optimal user scheduling and association o_{ij} and the associated number of users e_j with constants r' , r'_{ij} and r_{j0} . As $o_{ij} \in \mathbb{R}^{S \times V}$ and $e_j \in \mathbb{R}^V$, the variables in problem (25) can be rewritten as $\mathbf{G} := [o_{11}, \dots, o_{S1}, \dots, o_{1V}, \dots, o_{SV}, \dots, e_1, \dots, e_V]^T$ with $\mathbf{G} \in \mathbb{R}^{(S+1)V}$. Since there are no coupling terms for o_{ij} and e_j in the objective function in Eq. (25a), only the diagonal elements exist in the Hessian matrix. Thus, the Hessian matrix of Eq. (25a) with \mathbf{G} is

$$\mathbf{H}_1^{hessian} = \begin{bmatrix} 0 & & & & & \\ & \ddots & & & & \\ & & 0 & & & \\ & & & -\frac{1}{e_1} & & \\ & & & & \ddots & \\ & & & & & -\frac{1}{e_V} \end{bmatrix} \quad (35)$$

with $\mathbf{H}_1^{hessian} \in \mathbb{R}^{(S+1)V \times (S+1)V}$. Note that e_j is the number of effective load of BS j , which is the number of associated users according to definition 1 in Ref. [30]. Then, we have $e_j > 0$, and thus, $\mathbf{H}_1^{hessian}$ is a negative semidefinite matrix. Therefore, Eq. (25a) can be concluded as a concave function. Furthermore, the constraints in Eqs. (25b)-(25e) are all linear constraints. Then, we conclude that problem (25) is a convex problem.

REFERENCES

- [1] Y. Zeng, R. Zhang, and T. J. Lim, "Wireless communications with unmanned aerial vehicles: Opportunities and challenges," *IEEE Commun. Mag.*, vol. 54, no. 5, pp. 36–42, May 2016.
- [2] Y. Dong, M. Z. Hassan, J. Cheng, M. J. Hossain, and V. C. M. Leung, "An edge computing empowered radio access network with UAV-mounted FSO fronthaul and backhaul: Key challenges and approaches," *IEEE Wireless Commun.*, vol. 25, no. 3, pp. 154–160, Jun. 2018.
- [3] *Connecting the World From the Sky*. Facebook, Menlo Park, CA, USA, Mar. 2014.
- [4] S. Katikala, "Google project loon," *Sight, Rivier Acad. J.*, vol. 10, no. 2, pp. 1–6, 2014.
- [5] (Mar. 2014). *ABSOLUTE—Aerial Base Stations With Opportunistic Links for Unexpected and Temporary Events*. [Online]. Available: <http://www.absolute-project.eu/>
- [6] B. Galkin, J. Kibilda, and L. A. DaSilva, "Backhaul for low-altitude UAVs in urban environments," in *Proc. IEEE Int. Conf. Commun. (ICC)*, May 2018, pp. 1–6.
- [7] X. Lin, V. Yajnanarayana, S. D. Muruganathan, S. Gao, H. Asplund, H.-L. Maattanen, M. Bergstrom, S. Euler, and Y.-P. E. Wang, "The sky is not the limit: LTE for unmanned aerial vehicles," *IEEE Commun. Mag.*, vol. 56, no. 4, pp. 204–210, Apr. 2018.

- [8] S. Zhang, Y. Zeng, and R. Zhang, "Cellular-enabled UAV communication: Trajectory optimization under connectivity constraint," in *Proc. IEEE Int. Conf. Commun. (ICC)*, May 2018, pp. 1–6.
- [9] Q. Wu, Y. Zeng, and R. Zhang, "Joint trajectory and communication design for multi-UAV enabled wireless networks," *IEEE Trans. Wireless Commun.*, vol. 17, no. 3, pp. 2109–2121, Mar. 2018.
- [10] D. Yang, Q. Wu, Y. Zeng, and R. Zhang, "Energy tradeoff in ground-to-UAV communication via trajectory design," *IEEE Trans. Veh. Technol.*, vol. 67, no. 7, pp. 6721–6726, Jul. 2018.
- [11] Q. Wu and R. Zhang, "Common throughput maximization in UAV-enabled OFDMA systems with delay consideration," *IEEE Trans. Wireless Commun.*, vol. 66, no. 12, pp. 6614–6627, Dec. 2018.
- [12] Q. Wu, J. Xu, and R. Zhang, "Capacity characterization of UAV-enabled two-user broadcast channel," *IEEE J. Sel. Areas Commun.*, vol. 36, no. 9, pp. 1955–1971, Sep. 2018.
- [13] U. Challita, W. Saad, and C. Bettstetter, "Cellular-connected UAVs over 5G: Deep reinforcement learning for interference management," Jan. 2018, *arXiv:1801.05500*. [Online]. Available: <https://arxiv.org/abs/1801.05500>
- [14] M. Mozaffari, W. Saad, M. Bennis, and M. Debbah, "Efficient deployment of multiple unmanned aerial vehicles for optimal wireless coverage," *IEEE Commun. Lett.*, vol. 20, no. 8, pp. 1647–1650, Aug. 2016.
- [15] E. Kalantari, M. Z. Shakir, H. Yanikomeroglu, and A. Yongacoglu, "Backhaul-aware robust 3D drone placement in 5G+ wireless networks," in *Proc. ICC Workshops*, Paris, France, May 2017, pp. 109–114.
- [16] 3rd Generation Partnership Project; Technical Specification Group Services and System Aspects; System Architecture for the 5G System; Stage 2, documents 23.501, Version 15.0.0 Release 15, 3GPP, Jun. 2018.
- [17] C.-F. Liu, S. Samarakoon, and M. Bennis, "Fronthaul-aware software-defined joint resource allocation and user scheduling for 5G networks," in *Proc. IEEE Globecom Workshops (GC Wkshps)*, Dec. 2016, pp. 1–6.
- [18] C. Pan, C. Yin, N. C. Beaulieu, and J. Yu, "Distributed resource allocation in SDCN-based heterogeneous networks utilizing licensed and unlicensed bands," *IEEE Trans. Wireless Commun.*, vol. 17, no. 2, pp. 711–721, Feb. 2018.
- [19] I. Bor-Yaliniz and H. Yanikomeroglu, "The new frontier in RAN heterogeneity: Multi-tier drone-cells," *IEEE Commun. Mag.*, vol. 54, no. 11, pp. 48–55, Nov. 2016.
- [20] M. Hong, M. Razaviyayn, Z.-Q. Luo, and J.-S. Pang, "A unified algorithmic framework for block-structured optimization involving big data: With applications in machine learning and signal processing," *IEEE Signal Process. Mag.*, vol. 33, no. 1, pp. 57–77, Jan. 2016.
- [21] S. Boyd, N. Parikh, E. Chu, B. Peleato, and J. Eckstein, "Distributed optimization and statistical learning via the alternating direction method of multipliers," *Found. Trends Mach. Learn.*, vol. 3, no. 1, pp. 1–122, Jan. 2011.
- [22] M. Liyanage, A. Gurto, and M. Ylianttila, *Software Defined Mobile Networks (SDMN): Beyond LTE Network Architecture*. Hoboken, NJ, USA: Wiley, 2015.
- [23] V. Yazici, U. C. Kozat, and M. O. Sunay, "A new control plane for 5G network architecture with a case study on unified handoff, mobility, and routing management," *IEEE Commun. Mag.*, vol. 52, no. 11, pp. 76–85, Nov. 2014.
- [24] A. Gudipati, D. Perry, E. L. Li, and S. Katti, "SoftRAN: Software defined radio access network," in *Proc. ACM SIGCOMM Workshop Hot Topics Softw. Defined Netw.*, 2013, pp. 25–30.
- [25] C. Pan, C. Yin, N. C. Beaulieu, and J. Yu, "3D UAV placement and user association in software-defined cellular networks," *Wireless Netw.*, pp. 1–15, Jan. 2019. doi: [10.1007/s11276-018-01925-0](https://doi.org/10.1007/s11276-018-01925-0).
- [26] N. McKeown, T. Anderson, H. Balakrishnan, G. Parulkar, L. Peterson, J. Rexford, S. Shenker, and J. Turner, "OpenFlow: Enabling innovation in campus networks," *ACM SIGCOMM Comput. Commun. Rev.*, vol. 38, no. 2, pp. 69–74, Apr. 2008.
- [27] Open Networking Foundation (ONF). (2013). *OpenFlow-Enabled Mobile and Wireless Networks*. [Online]. Available: <https://www.opennetworking.org>
- [28] X. Song, C. Yin, D. Liu, and R. Zhang, "Spatial throughput characterization in cognitive radio networks with threshold-based opportunistic spectrum access," *IEEE J. Sel. Areas Commun.*, vol. 32, no. 11, pp. 2190–2204, Nov. 2014.
- [29] X. Cao, J. Xu, and R. Zhang, "Mobile edge computing for cellular-connected UAV: Computation offloading and trajectory optimization," in *Proc. IEEE 19th Int. Workshop Signal Process. Adv. Wireless Commun. (SPAWC)*, Jun. 2018, pp. 1–5.
- [30] Q. Ye, B. Rong, Y. Chen, M. Al-Shalash, C. Caramanis, and J. G. Andrews, "User association for load balancing in heterogeneous cellular networks," *IEEE Trans. Wireless Commun.*, vol. 12, no. 6, pp. 2706–2716, Jun. 2013.
- [31] S. Boyd and L. Vandenberghe, *Convex Optimization*. Cambridge, U.K.: Cambridge Univ. Press, 2004.
- [32] K.-Y. Wang, A. Man-Cho So, T.-H. Chang, W.-K. Ma, and C.-Y. Chi, "Outage constrained robust transmit optimization for multiuser MISO downlinks: Tractable approximations by conic optimization," *IEEE Trans. Signal Process.*, vol. 62, no. 21, pp. 5690–5705, Nov. 2014.
- [33] L. Liu, X. Chen, M. Bennis, G. Xue, and Z. Han, "A distributed ADMM approach for mobile data offloading in software defined network," in *Proc. IEEE Wireless Commun. Netw. Conf. (WCNC)*, Mar. 2015, pp. 1748–1752.
- [34] M. Chen, M. Mozaffari, W. Saad, C. Yin, M. Debbah, and C. S. Hong, "Caching in the sky: Proactive deployment of cache-enabled unmanned aerial vehicles for optimized quality-of-experience," *IEEE J. Sel. Areas Commun.*, vol. 35, no. 5, pp. 1046–1061, May 2017.
- [35] *Packings of Equal Circles in Fixed-Sized Containers With Maximum Packing Density*. Accessed: Mar. 2019. [Online]. Available: <http://www.packomania.com/>
- [36] D. P. Bertsekas, *Nonlinear Programming*. Nashua, NH, USA: Athena Scientific, 1999.



CHUNYU PAN received the Ph.D. degree from the School of Information and Communication Engineering, Beijing University of Posts and Telecommunications, Beijing, China. She has been a Lecturer with the School of Information and Communication Engineering, Beijing Information Science and Technology University, Beijing, since 2019. Her research interests include software-defined cellular networks, heterogeneous wireless networks, resource allocation, and mobility management in cellular networks.



JIRONG YI (S'16) received the B.Sc. degree in information and computing science from Harbin Engineering University, in 2015. He is currently pursuing the Ph.D. degree with The University of Iowa, USA, before which he was a Research Engineer with the Southern University of Science and Technology. His research interests include signal processing, deep learning, and mathematical optimization.



CHANGCHUAN YIN (M'98–SM'15) received the Ph.D. degree in telecommunication engineering from the Beijing University of Posts and Telecommunications, Beijing, China, in 1998. In 2004, he held a visiting position at the Faculty of Science, University of Sydney, Sydney, Australia. From 2007 to 2008, he held a visiting position at the Department of Electrical and Computer Engineering, Texas A&M University, College Station, USA. He is currently a Professor with the School of Information and Communication Engineering, Beijing University of Posts and Telecommunications. His research interests include wireless networks and statistical signal processing. He has served as a Technical Program Committee Member for various IEEE conferences. He was a co-recipient of the IEEE International Conference on Wireless Communications and Signal Processing Best Paper Award, in 2009.



JIAN YU received the B.E. degree in communication engineering from the University of Electronic Science and Technology of China, Chengdu, China, in 2010, and the Ph.D. degree in communication and information system from the Beijing University of Posts and Telecommunications, Beijing, China, in 2016. From 2013 to 2015, he was a Visiting Ph.D. Student with the University of Georgia Institute of Technology, Atlanta, USA. He is currently with Huawei Technologies Company Ltd. His research interests include cooperative communication, heterogeneous networks, and stochastic geometry theory in large-scale wireless networks.



XUEHUA LI received the Ph.D. degree in telecommunications engineering from the Beijing University of Posts and Telecommunications, Beijing, China, in 2008. She is currently a Professor and the Deputy Dean of the School of Information and Communication Engineering, Beijing Information Science and Technology University, Beijing. She is a Senior Member of the Beijing Internet of Things Institute. Her research interests include the broad areas of communications and information theory, particularly the Internet of Things, and coding for multimedia communications systems.

• • •